Novel rolltruded films: 4. Gas separation characteristics of rolltruded isotactic polypropylene

R. J. Ciora Jr and J. H. Magill*
Department of Chemical and Petroleum Engineering, University of Pittsburgh, Pittsburgh, PA 15261, USA
(Received 4 December 1992; revised 24 June 1993)

The gas separation characteristics of isotactic polypropylene (iPP) thin films produced via the rolltrusion solid-state processing technique have been studied in order to establish some principles underlying permeation/separation behaviour in relation to membrane texture. Ideal and actual separation factors have been determined for various processing temperatures and draw ratios to assess the impact of the unique triaxial morphology produced during rolltrusion. Previously, we have shown that this unique morphological texture can improve the gas permeability of iPP by reducing the diffusive pathway tortuosity and by increasing the microvoid content in the polymer. In this study we show that the separation factors generally improve in iPP as a result of rolltrusion processing. However, the actual separation factors for a mixture of CO_2 and N_2 are less than the ideal values for all processing conditions studied, although this difference decreases with increasing draw ratio and decreasing processing temperature. This discrepancy between the actual and ideal separation factors is attributed to a depression in the permeability of CO_2 in the mixture compared to the pure gas because of the presence of N_2.

(Keywords: rolltrusion; polypropylene; gas separation)

INTRODUCTION

Rolltrusion, a novel solid-state deformation process that combines the high compressive force of rolling with the high stress of drawing, can be used to produce thin films from most polymers, including those which are highly solvent resistant. These materials may be useful for a variety of high-temperature and/or harsh chemical environment membrane applications, two of which include vapour permeation and pervaporation operations for azeotrope breaking in dehydration and organic/organic separations[1,2] and equilibrium shifting in reversible vapour-phase reactions[3,4]. In this series of papers[5–7], we are investigating the quality of membranes produced via rolltrusion by examining the gas transport and separation characteristics of rolltruded isotactic polypropylene (iPP).

iPP has been chosen for these initial studies because of its processability to high draw ratios over a wide range of processing temperatures. Only gaseous penetrants have been chosen to minimize the polymer/penetrant interactions, thereby yielding a clearer indication of the specific effects of rolltrusion processing. Basic information obtained from such ideal systems will provide insight into the fundamental relationships between the transport coefficients and the rolltruded morphology.

Three factors commonly used to judge membrane quality are durability, permeability and selectivity. The high-performance, solvent-resistant polymers ultimately envisioned for membrane fabrication via rolltrusion, exhibit good mechanical stability as well as thermal and chemical resistance, which is often lacking in commonly used membrane polymers[8]. Furthermore, improvements in the wear resistance, dimensional stability and three-dimensional mechanical properties have been demonstrated with several homopolymers[9–17] as well as an ethylene/propylene copolymer[18], attesting to the durability and ruggedness of rolltruded films. Additionally, we have shown[5–7] conclusively that the dramatic declines in solubility and diffusivity, often observed in films processed by other solid-state techniques[19–25], are not encountered for rolltruded films. This is due to a decrease in the tortuosity and an increase in microvoid content of the rolltruded film, both of which serve to enhance the permeability of the amorphous matrix.

Therefore, to varying degrees, rolltrusion processing can improve polymer permeability and durability based upon gas transport and mechanical properties studies. In this paper, we investigate the effects of rolltrusion processing on the ideal separation factors of CH_4, N_2 and CO_2 in iPP. Variations in the actual separation factors of a mixture of CO_2 and N_2 are also examined and compared to the ideal values. To our knowledge this is the first reported study that considers actual separation factors for a film processed via a solid-state technique.

THEORY

Gas and vapour permeation through non-porous polymeric membranes occurs via the solution–diffusion mechanism[26]. The normalized throughput or permeability

* To whom correspondence should be addressed

0032-3861/94/05/0949–07

of penetrants in an amorphous polymer is defined as

$$P_0 = D_0 s_0 = \frac{Jh}{\Delta p} \quad (1)$$

where s_0 is the observed solubility, D_0 is the observed diffusivity, J is the flux, h is the membrane thickness and Δp is the pressure drop across the membrane. However, in semicrystalline polymers, the observed diffusivity and solubility are generally modified to reflect the presence of the crystallites such that

$$D_0 = \frac{\alpha_a D_a}{\tau \beta} \quad (2)$$

and

$$s_0 = \alpha_a s_a \quad (3)$$

where α_a is the amorphous volume fraction, τ is the diffusive pathway tortuosity, β is the amorphous chain immobilization constant, and D_a and s_a are the amorphous diffusivity and solubility respectively. All of these factors can be heavily influenced by rolltrusion[5–7]. In this paper, all reported transport coefficients are normalized by the amorphous volume fraction (e.g. D_0/α_a).

The ability of a membrane to separate components selectively from a mixture can be defined by the actual separation factor given by

$$\alpha_{i,j}^{\text{actual}} = \frac{y_i/y_j}{x_i/x_j} \quad (4)$$

where x and y are the feed and permeate mole fractions of species i or j. If there is little penetrant interaction between the components in the mixture and/or the membrane, then the apparent permeabilities of each component in the mixture, $P_{\text{mix},i}$, will be equivalent to their pure-component permeabilities, and equation (4) will reduce to a ratio of the pure-component permeabilities, specifically

$$\alpha_{i,j}^{\text{ideal}} = \frac{P_i}{P_j} \quad (5)$$

However, $\alpha_{i,j}^{\text{ideal}}$ is often not equivalent to $\alpha_{i,j}^{\text{actual}}$. In these instances, comparison of $P_{\text{mix},i}$ to the pure-component permeability can yield considerable insight into the penetrant/penetrant and polymer/penetrant interactions. Therefore, assuming the feed pressure is significantly greater than the permeate pressure, which was the case throughout this study, the apparent mixed-gas permeability of component i can be calculated using an equation of the form

$$P_{\text{mix},i} = \frac{y_i}{x_i} P_{\text{mix,tot}} \quad (6)$$

where $P_{\text{mix,tot}}$ is the total permeability of the mixture.

EXPERIMENTAL

Sample preparation

iPP billets obtained from Aristech Chemical Corporation were converted into films using the rolltrusion solid-state deformation technique described in recent papers[5,9–15]. Pertinent details of the rolltruded iPP films and processing conditions are shown in *Table 1*. The draw ratio (DR) is defined as the ratio of the initial to final film thickness. Final film thicknesses varied between 50 and 300 μm depending upon draw ratio and initial film thickness. The film prepared at a processing temperature (T_p) of 75°C and $DR \sim 8.7$ was deliberately stress-whitened or crazed, for comparison with the other films which were uncrazed. The crazed film has been included (as in the previous paper[7]) so as to provide some insight into the effect of 'void formation' (isolated) on the gas separation properties of rolltruded iPP.

Table 1 Pertinent characteristics of the rolltruded films shown as a function of processing draw ratio and temperature

Processing temperature (°C)	Draw ratio	X_c
Unprocessed	1.0	0.53
150	6.8	0.72
150	10.2	0.66
150	14.0	0.66
150	19.8	0.69
125	4.7	0.65
125	9.1	0.63
100	3.9	0.59
100	4.9	0.56
100	7.4	0.55
75	4.9	0.53
75 (crazed)	8.7	[a]
50	4.9	0.42

[a] Not available

Table 2 Properties of the gases used in this study

Gas	Diameter (nm) Kinetic[27]	Diameter (nm) LJ[28]	$(\varepsilon/k)_{LJ}$[28] (K)	V_c[28] ($cm^3\ mol^{-1}$)
CO_2	0.33	0.400	190	94.0
N_2	0.364	0.368	91.5	89.5
CH_4	0.38	0.382	137	99.0

Permeation/separation factor measurements

In addition to the gases considered in the previous study (CO_2, N_2 and CH_4), a gas mixture of CO_2 and N_2 (26.4% by volume CO_2) was also utilized, so that actual separation factor data could be obtained. Pertinent characteristics of these gases are given in *Table 2*. The transport coefficients, P_a, D_a and s_a, for the pure components and the CO_2/N_2 mixture were determined using the permeation apparatus already described[5]. Feed and permeate compositions were analysed via gas chromatography. All experimental runs in this study were conducted at a total feed pressure of 520 kPa and permeation temperature (T_d) in the range from 30 to 70°C. The permeate pressure was always kept below 10 torr which was negligible compared to the feed pressure. Under these conditions, the transport coefficients and separation factors were found to be independent of feed pressure from 172 to 1720 kPa.

RESULTS

Figure 1 shows $\alpha_{CO_2,N_2}^{\text{ideal}}$ and $\alpha_{CO_2,CH_4}^{\text{ideal}}$ plotted as a function of T_p and DR at a T_d of 40°C and a total driving pressure (Δp) of 520 kPa. The pure component permeabilities of CO_2, N_2 and CH_4, used in calculating $\alpha_{i,j}^{\text{ideal}}$ via

equation (5), were estimated from Arrhenius plots of the data obtained over the experimental T_d range of 30 to 70°C. Although the magnitude of the variation in $\alpha_{i,j}^{ideal}$ changes with T_d, specific trends observed at 40°C are typical of the entire T_d range. The crazed film is labelled CRAZED in this and other figures throughout the text.

The gases used in this investigation interact ideally with iPP so that the diffusivity and solubility are independent of penetrant pressure at the permeation conditions considered. As a result, $\alpha_{i,j}^{ideal}$ can be separated into two contributions, specifically the diffusive selectivity, $\alpha_{i,j}^{diff}$, and the solution selectivity, $\alpha_{i,j}^{soln}$, given by

$$\alpha_{i,j}^{ideal} = \frac{D_i}{D_j}\frac{S_i}{S_j} = \alpha_{i,j}^{diff}\alpha_{i,j}^{soln} \quad (7)$$

This factorization of $\alpha_{i,j}^{ideal}$ corresponds approximately to separation based upon penetrant size and penetrant/polymer interactions, respectively. Values of each factor for the various rolltruded films are given in *Table 3*. The X-fold change in each factor relative to the unprocessed film is shown in parentheses.

The actual separation factors for the CO_2/N_2 mixture, $\alpha_{CO_2,N_2}^{actual}$, are shown in *Figure 2* and are compared to $\alpha_{CO_2,N_2}^{ideal}$ values. The X-fold change in the mixture permeability of component i, $P_{mix,i}$, compared to the pure-component amorphous permeability, P_i, for CO_2 and N_2 are given in *Figure 3* where

$$\Delta P_i = \frac{P_{mix,i}}{P_i} \quad \text{for} \quad P_{mix,i} \geq P_i \quad (8)$$

or

$$\Delta P_i = \frac{P_i}{P_{mix,i}} \quad \text{for} \quad P_{mix,i} < P_i \quad (9)$$

Points above the dividing line in this figure indicate that the mixture permeability is greater than the pure component permeability and *vice versa*. The X-fold change is used here, as in other papers[6,7], so that an equivalent increase or decrease in ΔP_i is represented by an equivalent linear shift from the reference value of unity (the unprocessed film value).

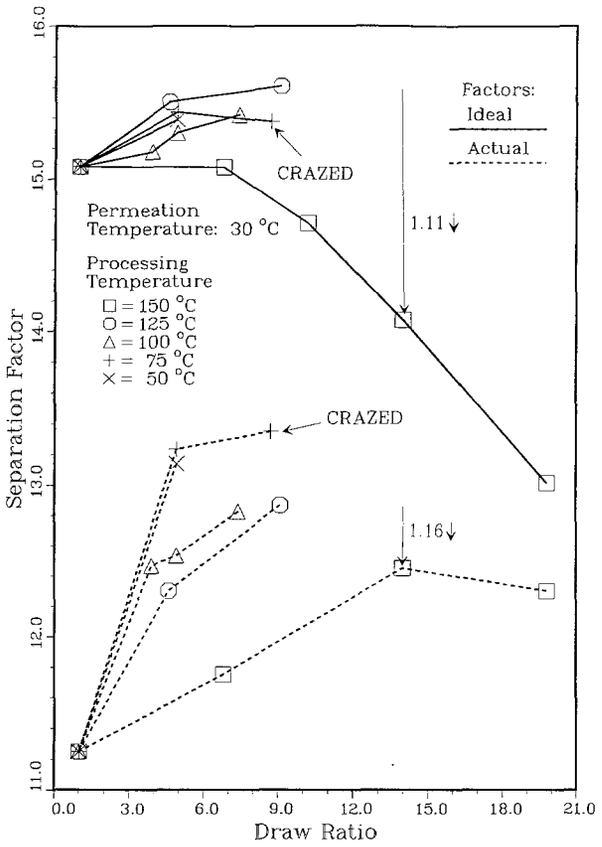

Figure 1 Ideal separation factors for CO_2/N_2 and CO_2/CH_4 in iPP plotted as a function of processing conditions. Note: Both sets of separation factors decline at 150°C relative to lower T_ps

DISCUSSION

Ideal separation factors

Variations in the diffusivity and solubility of CO_2, N_2 and CH_4 in iPP between the rolltruded and unprocessed films have been investigated extensively[6,7] and have been postulated to result from changes in the film tortuosity, microvoid content and the amorphous chain stiffness. These changes are summarized in *Table 4*. However, subtle differences between the transport coefficients of each penetrant were not examined in detail, since

Table 3 Diffusion and solution selectivities for CO_2/N_2 and CO_2/CH_4. The X-fold increase or decrease in each value compared to the unprocessed film is given in parentheses

T_p (°C)	DR	D_{CO_2}/D_{N_2}	S_{CO_2}/S_{N_2}	D_{CO_2}/D_{CH_4}	S_{CO_2}/S_{CH_4}
As-received	1.0	1.34(1.0)	11.2(1.0)	2.11(1.0)	2.98(1.0)
150	6.8	1.35(1.01↑)	11.1(1.01↓)	2.30(1.09↑)	2.98(1.0)
150	10.2	1.31(1.02↓)	11.2(1.0)	2.26(1.07↑)	3.00(1.01↑)
150	14.0	1.26(1.06↓)	11.2(1.0)	2.18(1.03↑)	2.98(1.0)
150	19.8	1.18(1.14↓)	11.0(1.02↓)	2.13(1.01↑)	2.95(1.01↓)
125	4.6	1.38(1.03↑)	11.2(1.0)	2.39(1.13↑)	2.62(1.14↓)
125	9.1	1.39(1.04↑)	11.2(1.0)	2.86(1.36↑)	2.64(1.13↓)
100	3.9	1.44(1.07↑)	10.6(1.06↓)	2.67(1.26↑)	2.69(1.11↓)
100	4.9	1.42(1.06↑)	10.7(1.05↓)	2.76(1.31↑)	2.71(1.10↓)
100	7.4	1.42(1.06↑)	10.8(1.04↓)	2.91(1.38↑)	2.62(1.14↓)
75	4.9	1.49(1.11↑)	10.3(1.09↓)	3.21(1.52↑)	2.55(1.17↓)
75 (crazed)	8.7	1.46(1.09↑)	10.6(1.06↓)	2.97(1.41↑)	2.45(1.22↓)
50	4.9	1.46(1.09↑)	10.5(1.07↓)	3.13(1.48↑)	2.56(1.16↓)

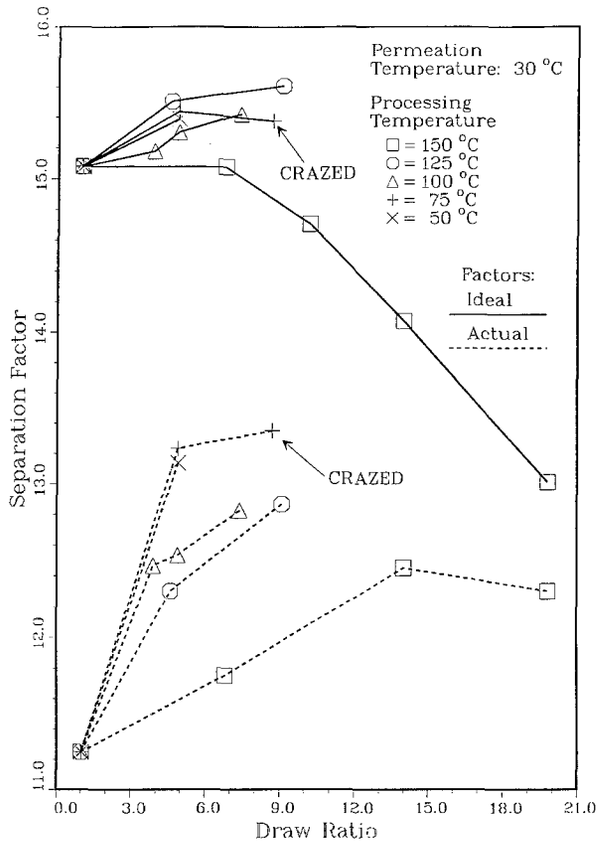

Figure 2 Ideal and actual separation factors for CO_2 and N_2 in rolltruded iPP plotted as a function of rolltrusion processing conditions

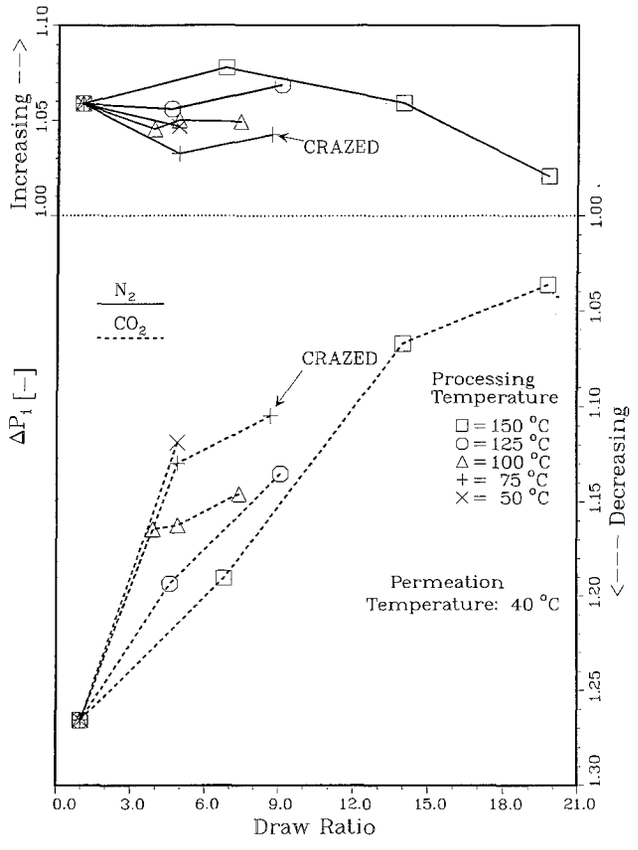

Figure 3 *X*-fold change in the amorphous permeability of CO_2 and N_2 in the mixed gas compared to the pure gas in rolltruded iPP plotted as a function of rolltrusion processing conditions

Table 4 Summary of the effects of rolltrusion processing on several key parameters condensed from previous gas transport results[6,7]

T_p (°C)	*DR*	Microvoid content	τ	*B* (or β)
150	1.0	1	1	1
150	6.8	++	−−−	+
150	10.2	1	−−	+
150	14.0	+	+	++
150	19.8	++	+	++
125	4.9	++++	−−−	++
125	9.1	+	+	+++
100	3.9	+	−−	++
100	4.9	++	−−	+++
100	7.4	+	+	+
75	4.9	++	−	+++
75	8.7	+++	+	+
50	4.9	+	++	++

Note: A plus (+) or minus (−) sign indicates an increase or decrease in the parameter relative to the value of the unprocessed film (1)

information of this kind is considered more appropriately in the context of the ideal separation factors or more specifically, the diffusive and solution selectivities.

Below $T_p = 150°C$ $\alpha^{ideal}_{CO_2,N_2}$ and $\alpha^{ideal}_{CO_2,CH_4}$ increase relative to the unprocessed film as shown in *Figure 1*. These increases can be attributed to improvements in the diffusive selectivity, $\alpha^{diff}_{i,j}$, of rolltruded iPP, which dominate the smaller yet significant declines in the solution selectivity, $\alpha^{soln}_{i,j}$, given in *Table 3*. *Table 3* also shows that $\alpha^{diff}_{CO_2,N_2}$ and $\alpha^{soln}_{CO_2,N_2}$ values are insensitive to alterations in the film draw ratio, although $\alpha^{diff}_{CO_2,N_2}$ may increase slightly as the T_p is lowered. These minor changes in $\alpha^{diff}_{CO_2,N_2}$ and $\alpha^{soln}_{CO_2,N_2}$ account for the limited dependence of $\alpha^{ideal}_{CO_2,N_2}$ on the processing conditions in the variously rolltruded films. In contrast, *Table 3* shows that $\alpha^{diff}_{CO_2,CH_4}$ is dependent upon the processing conditions compared to $\alpha^{diff}_{CO_2,N_2}$, although $\alpha^{soln}_{CO_2,CH_4}$ appears to be insensitive to both T_p and *DR*. These changes in the diffusive and solution selectivities are considered in terms of the rolltrusion morphology.

Differences between the diffusive selectivities of the rolltruded and unprocessed film are directly related to variations in the individual component diffusivities. Previously, changes in the diffusivity due to rolltrusion were attributed to variations in the amorphous-phase average chain separation, r_e, amorphous chain stiffness, β, diffusive pathway tortuosity, τ, and microvoid content[6,7]. However, it is doubtful that all of these parameters are important in a consideration of the enhancement of the diffusive selectivity.

First, it is unlikely that the production of microvoids can influence $\alpha^{ideal}_{i,j}$ substantially, since the microvoids do not constitute the continuous phase. If they were continuous, then a substantial reduction in selectivity would be observed, since Knudsen or even viscous flow would dominate the transport. Second, it is unlikely that the membrane tortuosity differs enough from one penetrant to another to affect the separation factors. This is reasonable, since the average cross-sectional area of the interlamellar amorphous regions (diffusive pathways) of the unprocessed and rolltruded films, as estimated by SAXS[12,13], is more than an order of magnitude greater than the diameter of the penetrants considered in this study. An improvement in the diffusive selectivity based

upon an increase in membrane tortuosity would require much narrower pathways of the order of the molecular diameter of the penetrants. Such pathways do exist in rolltruded iPP, but they are overwhelmed by others with much larger cross-sectional areas. It is therefore apparent that changes in microvoid content and τ are not expected to be fine enough or pervasive enough to influence the selectivity of these rolltruded films. Instead, alterations in the diffusive selectivity must be attributed to changes in β and r_e. These changes have been deduced from variations in the diffusive activation energies, E_d, of the penetrants[7], based upon the molecular theory of diffusion of Pace and Datyner[30,31].

We have shown previously that β increases substantially as a result of rolltrusion for T_p below 150°C. Furthermore, increases in β tend to dominate any physically realizable variations in the average amorphous chain separation below $T_p = 150$°C. A stiffer amorphous matrix, which results from rolltrusion, is expected to be more effective in hindering the diffusion of the largest penetrant. This accounts for the fact that the ideal separation factors increase and are more sensitive to changes in the processing conditions as the kinetic diameter (see *Table 2*) of the slow gas (N_2 and CH_4) increases.

In contrast to the diffusive selectivity, the solution selectivity decreases as the kinetic diameter of the slow gas increases for processing temperatures below 150°C as shown in *Table 3*. Intuitively, one would expect a parameter that models more closely the condensability of the penetrant (e.g. T_c or the Lennard-Jones potential $[(\varepsilon/k)_g]$) to better predict variations in solution selectivity which result from rolltrusion processing. However, neither the cohesive energy density of the polymer (CED_p) nor $(\varepsilon/k)_g$ are altered as a result of textural changes that arise from rolltrusion processing*. Hence, it is unnecessary that the *change* (increase or decrease) in the amorphous solubility and $\alpha_{i,j}^{soln}$, relative to the unprocessed film, should follow a trend in penetrant condensability.

The decrease in $\alpha_{i,j}^{soln}$ with increasing penetrant diameter of the slow gas is consistent with an increase in microvoid content in iPP deduced already from the transport results[6,7] (see *Table 4*). If gas sorption into a polymer is viewed as a two-step process, (i) hole formation and (ii) hole filling, then the increase in microvoid content should produce a decline in the hole formation energy, ΔH_h. This trend is similar in nature to the change in ΔH_h reported for glassy polymers that exhibit dual-mode behaviour[31]. According to Pace and Datyner[31], ΔH_h is approximately given by

$$\Delta H_h \propto \frac{CED_p^{3/4} B^{1/4} d^a}{r_e^{4.1}} \qquad (10)$$

where B is the chain-bending modulus (which is related to chain stiffness, β), d is the penetrant diameter, and a is approximately 1. Because of the dependence of ΔH_h on penetrant diameter, a localized expansion in the amorphous chain separation due to microvoid formation will produce a larger decline in ΔH_h (and ΔH_s) for the larger penetrants, and correspondingly a greater increase in solubility. Consequently, a larger decrease in $\alpha_{i,j}^{soln}$ results as the size of the slow gas increases, consistent with the results given in *Table 3*.

At $T_p = 150$°C $\alpha_{CO_2,N_2}^{ideal}$ decreases and $\alpha_{CO_2,CH_4}^{ideal}$ increases relative to the unprocessed film as *Figure 1* illustrates. However, both $\alpha_{CO_2,N_2}^{ideal}$ and $\alpha_{CO_2,CH_4}^{ideal}$ decline significantly when compared with results obtained for films prepared at lower T_p. As an example, $\alpha_{CO_2,N_2}^{ideal}$ and $\alpha_{CO_2,CH_4}^{ideal}$ decline roughly 1.11- and 1.16-fold, respectively, for the film processed at $T_p = 150$°C and $DR \sim 14$ relative to the film rolltruded at $T_p = 125$°C and $DR \sim 9.1$. Therefore, values of $\alpha_{i,j}^{ideal}$ at $T_p = 150$°C are considered relative to values obtained for films rolltruded at lower T_p.

Changes in the diffusive selectivity tend to dominate the relative decline in $\alpha_{i,j}^{ideal}$ at this T_p as at lower T_ps. As discussed earlier, $\alpha_{i,j}^{diff}$ is not expected to be influenced significantly by variations in the τ and microvoid content induced by rolltrusion. Instead, as at the lower T_p, variations in $\alpha_{i,j}^{diff}$ are consistent with the changes in r_e and β that have been deduced in a previous paper, based upon changes in E_d[6].

At $DR \sim 6.8$, the decline in the diffusive selectivity relative to the lower T_p can be attributed to a small decrease in the E_d of all three penetrants relative to the unprocessed film as reported previously[6]. In comparison, the E_d increases significantly for all rolltrusion conditions at $T_p < 150$°C. A decline in the E_d indicates that the amorphous matrix is more easily penetrated. Since the E_d is functionally similar to the ΔH_h, according to Pace and Datyner[30,31], a decline in the E_d should yield larger improvements in the diffusivity with increasing penetrant size. Hence, the diffusive or size selectivity is anticipated to decline at this T_p relative to lower temperatures which is verified in *Table 3*.

At higher draw ratios (>10), the depression in both α_{CO_2,N_2}^{diff} and $\alpha_{CO_2,CH_4}^{diff}$ at this T_p compared to films rolltruded at lower T_ps is expected to result from the large increase in the E_d for CO_2 compared to N_2 and CH_4 (see ref. 7). It follows that the ability of CO_2 to penetrate the amorphous matrix is hindered more effectively than the larger penetrants at these DRs. This behaviour may stem from a reduction in the plasticizing efficiency of CO_2. A similar decline in the plasticizing efficiency of CO_2 is not apparent for films produced at lower T_ps, based upon the ideal separation factors. However, changes in the actual separation factors for the mixture of CO_2 and N_2 do show apparent decreases in the plasticizing efficiency of CO_2 throughout the range of processing conditions investigated, as discussed below.

Actual separation factors

The ideal separation factors can be considerably larger than the actual separation factors, $\alpha_{CO_2,N_2}^{actual}$, as shown in *Figure 2*. Interestingly, the largest decline in $\alpha_{CO_2,N_2}^{actual}$ compared with the ideal values is observed for the unprocessed film. Furthermore, the increase in $\alpha_{CO_2,N_2}^{actual}$ with increasing DR and, to some extent, decreasing T_p is more distinct than with $\alpha_{CO_2,N_2}^{ideal}$. In fact, unlike $\alpha_{CO_2,N_2}^{ideal}$, $\alpha_{CO_2,N_2}^{actual}$ increases with DR at $T_p = 150$°C as shown in *Figure 2*. Clarification of these differences in the separation factors may become evident after the differences between the pure and mixture permeabilities of the individual components are examined.

The permeability of N_2 in the mixture, P_{mix,N_2}, (*Figure 3*) increases slightly compared with the pure-gas permeability as a result of rolltrusion processing,

* A change in CED_p would imply that the solubility of the polymer in a solvent could be altered by solid-state processing. Although it is conceivable that the rate of solvation would change (kinetic in origin), it is unlikely that the overall solubility would be altered

although P_{mix,N_2} appears to be independent of processing conditions. In contrast, P_{mix,CO_2} is substantially depressed in the unprocessed film and increases as the *DR* is raised and, to some extent, as the T_p is lowered.

The suppression of the mixture permeability of CO_2, P_{mix,CO_2}, may be attributed to a reduction in the plasticizing efficiency of CO_2 in the presence of N_2. *Figure 3* shows that ΔP_{CO_2} approaches 1.0 as the *DR* is raised and/or the T_p is lowered. This result indicates that the ability of N_2 to suppress or 'screen' CO_2 plasticization decreases for these processing conditions. On this basis, the ability of CO_2 to plasticize iPP (independent of the presence of N_2) probably decreases as a result of textural changes induced via rolltrusion processing and these changes attenuate the screening effect of N_2. However, it is not possible to determine from these data how the screening effect influences the solution or diffusive selectivities of $\alpha^{actual}_{CO_2,N_2}$. Information concerning the actual solubilities and diffusivities of these gases in the mixture are needed in order to complete this analysis. The current configuration of our permeation apparatus is not amenable to such determinations.

Values for $\alpha^{actual}_{i,j}$ are rarely reported for undeformed films and have never been cited for polymer films processed in the solid state. Instead, it is generally assumed that $\alpha^{actual}_{i,j}$ and $\alpha^{ideal}_{i,j}$ are equivalent for gases in rubbery polymers. However, the differences between $\alpha^{actual}_{CO_2,N_2}$ and $\alpha^{ideal}_{CO_2,N_2}$ found for a relatively inert polymer, like iPP, indicates that the 'screening' effects will be magnified in polymers that exhibit strong polymer/penetrant interactions. In fact, suppression of $\alpha^{actual}_{CO_2,N_2}$ at permeation temperatures above T_g is also observed in rolltruded poly(vinylidene fluoride)[32], suggesting that this result may be more common than is generally acknowledged. Screening in this way by an inert gas above the polymer T_g still needs to be further investigated.

Finally, it is important to examine the results for the rolltruded crazed film fabricated at $T_p = 75°C$ and $DR \sim 8.7$. This film displays one of the highest $\alpha^{actual}_{CO_2,N_2}$ values encountered in this investigation, even though it contains large *macro*voids that improve the overall penetrant throughput[7]. However, the separation results indicate that the macrovoids in the film are not the continuous phase. Instead, these large voids must be surrounded by a 'tight' non-porous amorphous matrix that is responsible for the measured high gaseous selectivity.

The symmetric non-porous rolltruded films considered in this study are not thin enough to compete economically with asymmetric films produced via phase inversion, especially for gas separation applications. However, the preliminary results for crazed iPP suggest that biphasic symmetric and possibly asymmetric membranes can be fabricated under suitable rolltrusion conditions. For films with sufficiently high macrovoid content, high permeability and selectivity may be achieved. In addition, rolltruded films may be useful for vapour permeation and pervaporation applications for which thin films are not a critical concern. Finally, rolltrusion processing does provide several advantages over solvent-based thin-film fabrication. These are (i) ease of film production, (ii) improved strength and better creep resistance, and (iii) the elimination of noxious solvents in film preparation to reduce health and safety concerns. In addition, rolltrusion processing eliminates the costs associated with solvent recovery. Hence, rolltrusion processing should be valuable for making thin films from solvent-resistant polymers, particularly for use as membranes in high-temperature and harsh chemical environments.

CONCLUSIONS

Ideal and actual separation factors have been determined for several gases in films of isotactic polypropylene fabricated via rolltrusion. Important conclusions are highlighted:

(1) For the ideal separation factors, the diffusants kinetic diameter is the most important factor in assessing the relative changes in both the diffusive and solution selectivities and therefore the ideal separation factors. Furthermore, it has been found that $\alpha^{diff}_{i,j}$ increases and $\alpha^{soln}_{i,j}$ decreases with kinetic diameter, consistent with the molecular theory of diffusion of Pace and Datyner[30,31].

(2) Over the entire range of rolltrusion processing conditions that produce varying degrees of film texturing, the actual separation factors for the CO_2/N_2 mixture were found to be depressed relative to the ideal values, due to the reduced permeability of CO_2 in the mixture. This reduction has been attributed previously to 'screening' of the plasticizing efficiency of CO_2 by N_2.

(3) It has been demonstrated that controlled crazing of the films does not adversely affect its separation properties and improves the permeability.

ACKNOWLEDGEMENTS

The authors would like to thank the Aristech Chemical Corporation for providing the isotactic polypropylene billets used in processing films for this experimental work.

REFERENCES

1 Goldblatt, M. E. and Gooding, C. H. *AIChE Symp. Ser.* 1986, **82** (248), 51
2 Rautenbach, R. and Albrecht, R. 'Membrane Processes', John Wiley and Sons, New York, 1989
3 Ilias, S. and Govind, R. *AIChE Symp. Ser.* 1989, **82** (268), 18
4 Doshi, K. J., Werner, R. G. and Mitariten, M. J. *AIChE Symp. Ser.* 1989, **85** (268), 53
5 Ciora, R. J. and Magill, J. H. *J. Polym. Sci., Polym. Phys. Ed.* 1992, **30**, 1035
6 Ciora, R. J. and Magill, J. H. *J. Polym. Sci., Polym. Phys. Ed.* in press
7 Ciora, R. J. and Magill, J. H. in preparation
8 Dyson, R. W. (Ed) 'Engineering Polymers', Chapman and Hall, New York, 1990
9 Sun, D. C., Berg, E. M. and Magill, J. H. *Polym. Eng. Sci.* 1989, **29**, 715
10 Sun, D. C., Berg, E. M. and Magill, J. H. *Polym. Eng. Sci.* 1990, **30**, 635
11 Sun, D. C. and Magill, J. H. *J. Polym. Sci., Polym. Lett. Ed.* 1987, **34**, 2337
12 Sun, D. C., Magill, J. H. and Lin, J. S. American Physical Society, New Orleans Meeting, March 21–25 1988
13 Shankernarayanan, M. J., Magill, J. H. and Lin, J. S. American Physical Society (DHPP), New York Meeting, March 1987
14 Sun, D. C. 'Preparation and Modeling of Doubly Oriented Polymers', PhD dissertation, University of Pittsburgh, 1988
15 Shankernarayanan, M. J., Sun, D. C., Kojima, M. and Magill, J. H. *Int. Polym. Proc.* 1987, **1**, 66
16 Voss, H., Magill, J. H. and Friedrich, K. *J. Appl. Polym. Sci.* 1986, **33**, 1745
17 Voss, H., Magill, J. H. and Friedrich, K. *J. Appl. Polym. Sci.* 1987, **34**, 177
18 Lin, C. C., Kojima, M. and Magill, J. H. *J. Mater. Sci.* 1992, **27**, 5849
19 Peterlin, A., Williams, J. L. and Stannett, V. *J. Polym. Sci. (A-2)* 1967, **5**, 957

20 Williams, J. L. and Peterlin, A. *J. Polym. Sci. (A-2)* 1971, **9**, 1483
21 Yasuda, H. and Peterlin, A. *J. Appl. Polym. Sci.* 1974, **18**, 531
22 DeCandia, F., Russo, R., Vittoria, V. and Peterlin, A. *J. Polym. Sci., Polym. Phys. Ed.* 1982, **20**, 269
23 Wang, L. H. and Porter, R. S. *J. Polym. Sci., Polym. Phys. Ed.* 1984, **22**, 1645
24 Choy, C. L., Leung, W. P. and Ma, T. L. *J. Polym. Sci., Polym. Phys. Ed.* 1984, **22**, 707
25 Vittoria, V., DeCandia, F., Capodanno, V. and Peterlin, A. *J. Polym. Sci., Polym. Phys. Ed.* 1986, **24**, 1009
26 Kesting, R. E. 'Synthetic Polymeric Membranes: A Structural Perspective', 2nd Edn, John Wiley and Sons, New York, 1985
27 Breck, D. W. 'Zeolite Molecular Sieves', John Wiley and Sons, New York, 1974
28 Bird, R. R., Stewart, W. E. and Lightfoot, E. N. 'Transport Phenomenon', John Wiley and Sons, New York, 1960
29 Bixler, H. J. and Sweeting, O. J. 'Barrier Properties of Films' in 'The Science and Technology of Polymer Films', Wiley Interscience, New York, 1971, Vol. 2, pp. 1–61
30 Pace, R. J. and Datyner, A. *J. Polym. Sci., Polym. Phys. Ed.* 1979, **17**, 453
31 Pace, R. J. and Datyner, A. *J. Polym. Sci., Polym. Phys. Ed.* 1980, **18**, 1169
32 Ciora, R. J. and Magill, J. H. unpublished results

NOMENCLATURE

B	Chain bending modulus (J nm mol^{-1})
CED_p	Cohesive energy density of the polymer (J cm^{-3})
d_i^k	Kinetic diameter of penetrant (nm)
$d_{L,J}$	Lennard-Jones diameter of the penetrant (nm)
d_o	$d + r^* - r_e$ (nm)
D_a	Amorphous diffusivity (cm^2 s^{-1})
D_o	Observed diffusivity (cm^2 s^{-1})
DR	Draw ratio (−)
E_d	Diffusive activation energy (kJ mol^{-1})
h	Membrane thickness (μm)
ΔH_s	Heat of solution (kJ mol^{-1})
J	Flux (cm^3{STP} cm^{-2} s^{-1})
P_a, P_i	Amorphous permeability (cm^3{STP}cm cm^{-2} s^{-1} cmHg^{-1})
P_o	Observed permeability (cm^3{STP}cm cm^{-2} s^{-1} cmHg^{-1})
$P_{mix,i}$	Mixture permeability of component i (cm^3{STP} cm cm^{-2} s^{-1} cmHg^{-1})
$P_{mix,tot}$	Total mixture permeability (cm^3{STP}cm cm^{-2} s^{-1} cmHg^{-1})
ΔP_i	X-fold change in mixture *versus* pure permeability, component i (−)
Δp	Pressure drop (cmHg)
r_e	Equilibrium chain separation (nm)
s_a	Amorphous solubility (cm^3{STP} cm^{-3} cmHg^{-1})
s_o	Observed solubility (cm^3{STP} cm^{-3} cmHg^{-1})
T_p	Processing temperature (°C)
T_d	Permeation temperature (°C)

Greek letters

α_a	Amorphous volume fraction (−)
$\alpha_{i,j}^{actual}$	Actual separation factor (−)
$\alpha_{i,j}^{ideal}$	Ideal separation factor (−)
$\alpha_{i,j}^{diff}$	Diffusive selectivity or separation factor (−)
$\alpha_{i,j}^{soln}$	Solution selectivity or separation factor (−)
β	Chain immobilization factor (−)
$(\varepsilon/k)_g$	Lennard-Jones potential of the gas (K^{-1})
τ	Tortuosity (−)